Biogeochemistry (2013) 112:197–208
DOI 10.1007/s10533-012-9716-1

Large-scale spheroidal redoximorphic features around plinthite nuclei in Orinoco River sediments reflect mean seasonal fluctuation in river stage and ENSO-related anomalies

R. Herrera · N. Chacón

Received: 31 May 2011 / Accepted: 12 February 2012 / Published online: 7 April 2012

Abstract In sediments emerging on the scarp of Lower Orinoco River, Venezuela, we have discovered and studied large (0.5 m) features formed by a plinthite nucleus surrounded by evenly spaced concentric spheroidal structures of iron oxides separated by depletion zones. These features are located in sediments subjected to the mean annual river fluctuation (approx. 14 m) and hence are submerged for several months each year. To the best of our knowledge, structures like these have never been reported or studied. The nuclei and concentric ring formations found in the Orinoco sediments represent an extreme case of regular currently alternating redox conditions. Here we show that the concentric ferric rings surrounding the nuclei could be the result of repeated cycles of diffusion of ferrous ions during flood and subsequent precipitation as ferric oxide during the dry period, thus reflecting the seasonal fluctuation in river level. Our results are consistent with a simple proposed model of ferrous iron diffusion/oxidation according to the flood/dry intervals imposed by river dynamics. This paper is a contribution toward understanding these redoximorphic features (RFs) by: (1) describing their composition and mineralogy; (2) suggesting a possible mode of their formation using the switch to reducing conditions and diffusion of soluble Fe during flood, and its subsequent oxidation and hence immobilization and partial crystallization once exposed to the air; (3) by confirming how this theoretical approach fits the actual pattern of river hydrology in Orinoco, both under average conditions, and as modified by climatic extreme conditions influenced by the El Niño/La Niña Southern Oscillation (ENSO) affecting the ratio of flood/emergence.

Keywords River sediments · River dynamics · Redox processes · Spheroidal structures

R. Herrera · N. Chacón
Centro de Ecología, Instituto Venezolano de Investigaciones Científicas, Apdo. 20632, Caracas 1020A, Venezuela

Present Address:
R. Herrera (✉)
Departamento de Ingeniería Hidráulica y Medio Ambiente, Universidad Politécnica de Valencia, Camí de Vera s/n, 46022 Valencia, Spain
e-mail: rherrera@upvnet.upv; rherrera.valencia@hotmail.com

Introduction

Ferruginous nodules, crusts, and structures usually associated with laterites or plinthites are common features in many tropical and subtropical soils and sediments. Their formation is thought to be related to alternating wetting and drying cycles (Lelong 1966; Stolt et al. 1994). Although it is usually accepted that these redoximorphic features (RF) are a function of redox processes that result in the relative concentration

or depletion zones of iron (Fe), the actual mechanism through which the alternation of reducing and oxidizing conditions gives rise to redoximorphic structures in soils and sediments is still poorly understood (Sivarajasingham et al. 1962; van Wambeke et al. 1983; Vepraskas 1992; Vepraskas and Faulkner 2000; Wiederhold et al. 2007; Chan et al. 2004; 2007). In seasonally exposed sediments in the scarp of the northern banks of Lower Orinoco River, Venezuela (Fig. 1) we have observed unusually large (up to 0.5 m diameter) concentric three-dimensional (3-D) structures formed by a plinthite nucleus surrounded by evenly spaced concentric reddish rings of iron oxides with depletion zones between them (Fig. 2). The bare, nearly flat sediment surface where most of these RFs were found is located between 16.9 and 17.4 m a.s.l., which is approximately 5 m above the minimum average river-level fluctuation and some 9 m below the average high water mark. Therefore, the surface where the RFs were found is under water for an average of 212 days each year; the rest of the year, when the river level is lower, they are exposed to the air. This change from conditions presumed to be reducing to oxidizing conditions occurs abruptly since the water level drops rapidly in October–January, typically approximately 10 cm per day. Oxidation should thus proceed uninterrupted since little or no rain usually falls at the mid-dry season (less than 3 % of annual total precipitation falls between December and March). To the best of our knowledge, structures such as these have never been reported or studied in tropical rivers.

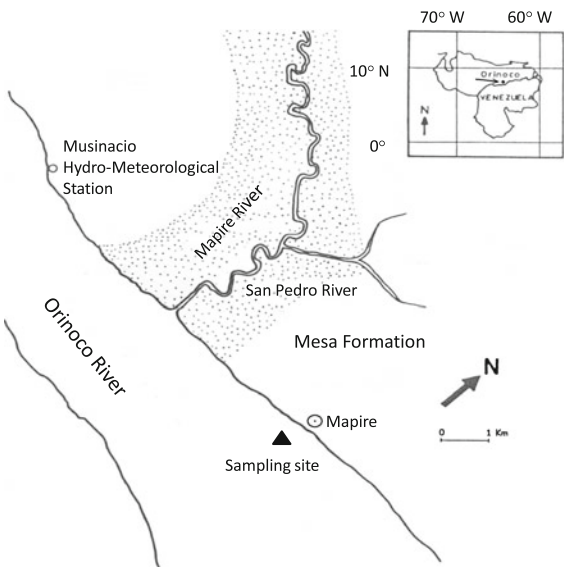

Fig. 1 Location map indicating the sampling site in Lower Orinoco River, Venezuela and its relative position in the left-bank scarp. The Mesa Formation and the floodplain (*dotted area*) are also shown (modified from Rodríguez-Altamiranda et al. 2011)

Spicar (2004) described a large concentric ring structure in exposed sandstone sediments in Dalarna, Sweden that could be attributed to iron reduction and probably with associated biological processes. Whether this structure occurs only at the surface of the sandstone is not clear. Asikainen and Werle (2007) reported ferromanganese nodules that measure up to 46 cm in diameter in sediments of shallow lakes of New Hampshire. Thompson et al. (2006a, b) and Fimmen et al. (2008) hypothesize the existence of a potent weathering process operative in upland subsoils where water-table fluctuations occur imposing redox cycles of organic carbon (C) and Fe, leading to the formation of reddish and light banding (Liesegang banding). Chan et al. (2004, 2007) studied and modeled the formation relict spheroidal concretions in Utah deserts, which can show internal layering of iron oxide concentration and depletion zones. Barge et al. (2011) compared the experimental formation of periodic precipitates in porous media with diagenetic processes in natural environments.

The redoximorphic features and ferromanganese nodules that have been reported in the literature generally show little physical resemblance to the ones we have discovered in exposed sediments in the scarp of Orinoco River, Venezuela. However, in the RFs found in Orinoco, the color, banding, and depletion zones are reminiscent of redoximorphic structures and mottling in soil profiles subjected to a fluctuating water table (Wiederhold et al. 2007). Their spheroidal structure and banding shows some similarities to much smaller relict concretions reported by Chan et al. (2004) and Gasparatos et al. (2005). They differ in size and show a striking regularity of concentric depletion and reddish 3D layers surrounding the nucleus, especially because they currently remain under water for a prolonged period, emerging during low water stages following the river-stage dynamics in a quasi-regular fashion.

Although it is generally accepted that redoximorphic features are related to redox processes during alternating wetting/drying cycles, little is still known about the mechanisms of iron mobility in accretionary processes.

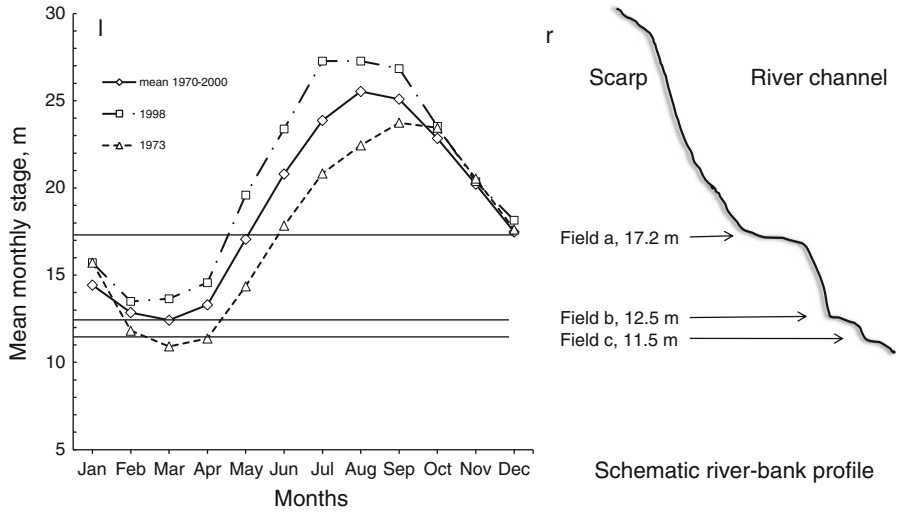

Fig. 2 *Left* Mean monthly river stage (average 1970–2000), mean monthly river stage for a dry year (1973) and mean monthly river stage for a wet year (1998). *Right* Schematic profile of the left bank of the Orinoco River at the site. Relative positions of the three fields (*a–c*) where redoximorphic features were observed. Relative height (*arrows*) for fields *a–c* is given at the same vertical scale as in the *left* figure

Small-scale banding (<5 mm) due to iron migration in soils away from a source has been described and modeled (Kirk et al. 1990). A very fast rate of accretion (0.26 mm year^{-1}) of fresh water nodules in lake bottoms was reported by Asikainen and Werle (2007), while other studies of freshwater nodules report accretion rates of only 0.003 mm year^{-1} (Sommers et al. 2002). In soil profiles with fluctuating water tables significant enrichments of heavy Fe isotopes of about 0.3 ‰ in δ^{57}Fe were found in total soil digests of Fe-depleted zones compared with bulk soil samples; these were explained by the preferential removal of light isotopes, presumably during microbial-mediated Fe oxide dissolution under anoxic conditions (Wiederhold et al. 2007). Chan et al. (2006) also found relative discrimination against the heavier Fe isotopes, presumably due to biological processes during the formation of iron-rich spherules. Iron isotope fractionation is thus linked to Fe transformations in redoximorphic soils and in concretions, revealing the greater mobility of lighter Fe isotopes during pedogenesis or the development of RFs.

The Orinoco suspended sediments are a mix of distant Guayana Shield and Andean sources (Lewis and Saunders 1989; Paolini 1995). The local source of both the light-colored consolidated sediment in the scarp of Lower Orinoco and the iron-rich nuclei near Mapire (Fig. 1) could be the Pleistocene Mapire and Musinacio Mesa Formation, just north of our experimental site. Carbón and Schubert (1994) provide a detailed description of alluvial sediments where, as a result of erosion, deep canyons have been formed by scarp retreat, revealing unconsolidated sediments and the presence of hardened sands preserved by iron oxides. Rounded or columnar fragments of plinthite from this formation could be one source of the observed nuclei.

The Orinoco River basin in northern South America lies between 1° 30′ and 10° 20′N; 74° 45′ and 59° 30′W and is thought to receive the precipitation originating from the prevailing NE trade winds from the Atlantic and Caribbean following the transit of the Inter-tropical Convergence Zone (ITCZ). Orinoco is the world's third largest river in terms of water discharge, with annual water-level fluctuations reaching an average of approximately 14 m in its lower course. Unusual conditions, such as wetter or drier periods associated with the El Niño/La Niña Southern Oscillation (ENSO), can modify this pattern (Poveda and Mesa 1997; Labat et al. 2005; Poveda et al. 2006; Nieto et al. 2008). García and Mechoso (2005) found that the two largest tropical rivers in South America; i.e. the Amazon and Orinoco, show a tendency towards slightly increased streamflows during cold events and a smaller impact of warm events. Since the former drainage system lies entirely in the Southern Hemisphere and the latter in the Northern Hemisphere, these anomalies occur at different times during the year. They also report quasi-oscillations in streamflows with El Niño-like periodicities.

The main question addressed in this paper is the role of the quasi-regular alternation of oxic and anoxic conditions imposed by annual river-level variation on the formation of the redoximorphic structures discovered

in the exposed sediments in the scarp of the Orinoco River banks. To answer this question, the Fe concentrations obtained from the nuclei and in the individual concentric rings of the studied structures are related to a hypothetical accretionary mode of formation driven by the river dynamics. In this study, we hypothesized that if these structures were to be the result of periodic alternating redox conditions driven by average river dynamics, they should also respond to changes in the ratio of flood:emergence influenced by such climatic phenomena as ENSO. These RFs are thought to be the product of a current phenomenon, while most other cases of similar structures are relict, and the alternating redox conditions during their formation should be inferred.

Materials and methods

Site description

Orinoco River shows a mono-modal hydrogram with a maximum in late August or early September and a minimum in mid March. River level is measured twice daily at the Musinacio hydro-meteorological Station near Mapire, Venezuela (Fig. 1). The average monthly river-level fluctuation between mean river maxima and minima for the period 1970–2000 is 13.5 m (http://www.inameh.gob.ve), varying between 10.1 and 15.6 m in very dry and wet years, respectively. The difference between the absolute minimum and maximum for the same period is over 17 m. In August river depth can reach over 30 m (ORE/HYBAM—6th Orinoco Campaign 2007). The river surface slope between the Musinacio Station and the following station downstream at Ciudad Bolívar, 130 km distant, is <0.01 %. Figure 2 shows that, on average, river level attains its minimum in March and its maximum in August. In very wet years, such as 1998, river level drops at a slower rate as the dry season progresses; during the wet season, the river level rises faster and peaks a month earlier, i.e., in July. In contrast, during very dry years, as in 1973, the rate at which the level of the river drops is more pronounced between November and March; once the rainy season starts, the rise is delayed, peaking a month later, i.e., in September. Although local groundwater inflow from the Mesa Formation just north of Mapire cannot be ignored, we suggest that this may have only a minor influence on the processes of RF formation due to the very large discharge of the Orinoco River during floods ($>6 \times 10^4$ m^3 s^{-1}). Thomaz et al. (2007) consider the influence of the hyporrheic zone to be significant during the low-water period in the Orinoco and Amazonas Rivers while during floods, due to the sheer magnitude of the main stream discharge, it acts as a homogenizing force by increasing connectivity in these large-scale river systems.

We have observed that during the low-water phase, light-colored, bare sediments emerge as nearly flat terraces in the scarp on the northern banks of Orinoco River, close to the village of Mapire, Venezuela. In one of these terraces we discovered horizontally disposed arrays of reddish concentric rings surrounding darker nuclei separated by lighter depletion zones (Fig. 3). These structures vary in size, with the largest being over 0.5 m in diameter. The concentric rings surrounding the nuclei are generally rounded in shape, although in some cases, due to cracks or irregularities in the sediment, they can be skewed. They do not show a preferential elongation in the same direction of the river flow. These structures have been repeatedly observed every dry season since 1988, with no apparent changes from year to year. The matrix in which these features are embedded, forming a series of spheroidal reddish bands, is a compact light-colored clay material containing sand-sized grains (approx. 33%). The nearly flat surface of the sediment terrace where these structures appear is located at between 16.9 and 17.4 m a.s.l., using as a reference the nearby Mapire River gauging station (Musinacio) on the left margin of Orinoco at 7° 43′20.1″N, 64° 42′48.9″W. The location of the RFs that we have studied within the bounds of the annual river fluctuation is shown in Fig. 2. Further below in the same scarp, during the low-water period (March–April), we have observed similar structures in other nearly horizontal surfaces emerging at 12.5 and 11.5 m a.s.l. The relative location of these two additional sediment surfaces is depicted in Fig. 2, right. These ring structures also surround plinthite nuclei, and although the concentric rings are similar in color, they tend to show narrower rings that are more widely spaced. As a consequence of their relative position, each of these structures remains flooded for periods ranging from over 11 months to almost 3 years. In the emergent phase they become completely dry for shorter periods since this

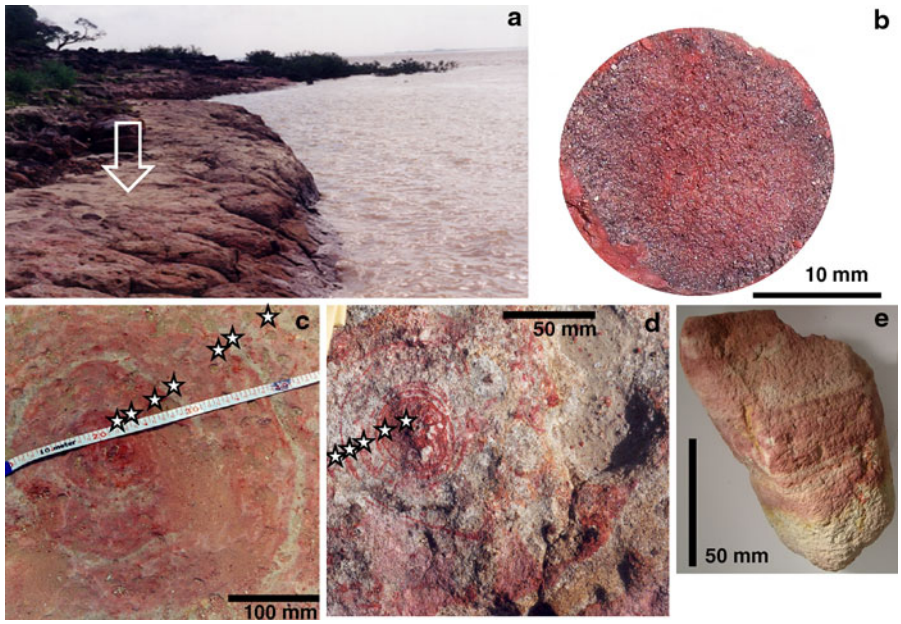

Fig. 3 **a** Photo of Orinoco River sediment surface (*arrow*) where redoximorphic features can be observed when the water stage drops (December–May) below this level. **b** Close-up (×10) of plinthite nucleus surface exposed on sediment; notice reddish undifferentiated core and darker corona (see text). **c**, **d** Field photos of the largest and smallest redoximorphic features studied where quasi-concentric ring structures can be seen. *Stars* Approximate sampling points. **e** Banded structure of a sediment block extracted from a pit just below a redoximorphic feature. (color figure online)

occurs during the peak of the dry season when the river level is at its lowest.

Characterization of redoximorphic features

Five of these plinthite nuclei and their surrounding structures were measured in situ in the sediment field located between 16.9 and 17.4 m a.s.l. (Fig. 3, Field a). The diameter of the nucleus varied between 6 and 20 mm. Samples of each nucleus and successive light and reddish rings were taken using a steel impact borer (diameter 5 mm) to a depth of 10–15 mm, and the distance of each sampling point to the surface of the nucleus along a single radius was noted (Fig. 3c, d). Munsell color was taken from each sample after wetting. In four of the redoximorphic structures there were between two and four distinct reddish rings separated by distinct depletion zones; a smaller structure showed a single ring that was about 10 cm in outer diameter. This latter ring showed narrow internal banding at short intervals (approx. 0.7 cm) (Fig. 3d). When a pit was excavated just below one of the sampled RFs, we observe that the stained sediment bands on the surface corresponded to concentric shells forming a 3-D structure (Fig. 3e). Extracting a whole RF was, however, not feasible due to their large size.

Each sample was dried, ground in an agate mortar, and sieved to <2 mm. Total iron (Fe_T) was obtained from a complete digestion of the sample (0.5-g aliquots) in hydrofluoric acid (Jackson 1958) and then determined by atomic absorption spectrophotometry (AAS).The results obtained for each sample were normalized as the ratio of Fe concentration between the individual concentric ring and the concentration in the corresponding nucleus. Amorphous (Fe_o) and crystalline (Fe_d) forms of Fe were separated from duplicate 1.0-g aliquots according to Borgaard (1979) and Mehra and Jackson (1960), and their Fe concentration was analyzed by AAS. Texture was determined in a selection of samples of nucleus, reddish rings, and lighter colored ring materials after grinding in an agate mortar and sieving to <2 mm using a Bouyoucos hydrometer in a suspension of 20 g of material in 1 L of water (Gee and Bauder 1986). Porosity was measured in five undisturbed nuclei weighing 3–5 g and eight undisturbed clods of the sediment matrix taken away from the RFs, each weighing 0.3–3 g. The nuclei and clods were first saturated with water for

24 h, following which, following the draining off of free water, the samples were placed on absorbent filter paper and exposed to a gentle air-current. The saturated weight and oven-dry weight (105 °C) were measured to the nearest 0.001 g. Porosity was calculated assuming the water density at 25°C to be 0.9971 g cm^{-3} and the density of minerals to be 2.81 and 2.65 g cm^{-3} in iron-rich nuclei and sediment, respectively. X-ray diffraction analysis using CoKα radiation was performed on the <2-μm fraction separated by sonication and collected by centrifugation. Samples of nodule and reddish and light-colored ring materials were mounted on glass plates and analyzed from 11°–67° 2θ. Diffraction peaks were assigned using pure mineral controls for comparisons.

Results and discussion

Table 1 shows the distance from the nucleus surface, total Fe, relative concentrations for each of the five redoximorphic structures sampled in Field a (Fig. 3) as well as the relative proportions of amorphous and crystalline iron oxides and Munsell color. For each ring sample, an indication of whether it is a depletion zone (*D*) or concentration zone (*C*) is also given based on the visual aspect as well as Munsell color. The Fe_2O_3 concentration in the nuclei of the five structures studied varied between 3 and 8 %, with an average of 5.51 ± 1.87 %. As distance increases from the nucleus, total Fe drops to about one-fifth of the concentration in the nucleus, but it shows alternating higher and lower values corresponding to reddish (*C*) and lighter (*D*) zones. Although the RFs vary in size, the spacing between the outer limit of consecutive reddish rings is quite even, close to 5.5 cm. The ratio Fe_o/Fe_d is nearly always <1, thereby indicating a general predominance of crystalline iron oxides. It is noteworthy that outer rings seem to be predominantly crystalline iron oxides in comparison with the nucleus. Textural analysis showed that the matrix of the sediment is clay (54 %) with a proportion of sand (33 %). Textural differences between the reddish rings, depletion zone, and sediment matrix materials were negligible. The porosity (volume) of undisturbed nuclei was 0.25 ± 0.05 ($n = 5$), while that of undisturbed sediment clods was on average 0.45 ± 0.06 ($n = 8$). The porosity value for the nuclei is within the range of that of reported for concretions in Navajo sandstones, Utah (Chan et al. 2004; Parry 2011). A strong local reduction in porosity in the dark outer rind of these nuclei (Fig. 3b), could, however, be expected due to goethite filling the pore-space (Parry 2011). Our estimate of the sediment matrix porosity is higher than the reported value for Navajo Sandstone but is of the same order as that reported by Atkins and McBride (1992) for river and beach sediments. The mineralogy of the sediment matrix was dominated by kaolinite and quartz, while in the nodules and reddish rings, in addition to kaolinite and quartz, hematite and goethite were also identified by X-ray diffraction analysis. In this assessment we homogenized the nuclei samples; therefore, no distinction could be made between the reddish core and the outer dark rind in terms of Fe content or mineralogy (Fig. 3b).

In Fig. 4, we have plotted the relative concentrations of Fe_2O_3 to those of the corresponding nuclei for the five structures studied, as a function of the radial distance from the nucleus surface. We can observe a sharp drop in the relative concentration C/C_0, which reaches an asymptotic value with distance (>30 cm). However, this apparent exponential decay seems to be modulated at shorter distances in a quasi-regular fluctuation up to some 25 cm away from the nucleus surface. The maxima correspond to concentration zones (*C*) and the minima to depletion zones (*D*). As a first approximation, we used a cubic smoothing spline passing by $C/C_0 = 1$ (Fig. 4, curve a). Upon observing that the general shape of the curve seems to follow an exponential decay as a general trend, we then calculated the best fit, adding a sinusoidal term to account for the already noted quasi-regular fluctuations. This is given as curve b in Fig. 4 that can be expressed as:

$$C/C_0 = b_1 e^{-kt} + b_2 \sin(\omega t + \delta) + b_3 \quad (1)$$

where C is the measured Fe_2O_3 concentration at distances (in centimeters) from the nucleus surface; C_0 is the Fe_2O_3 concentration measured in the corresponding nucleus; t is the time lapsed (in seconds), k is the decay constant, and ω and δ are the angles (in radians) by which to obtain the best fit for the experimental points. The best fit was found to occur at the following values: $b_1 = 0.7$; $k = 0.5276$; $\omega = 1.1687$ rad; $\delta = 2.7745$ rad; $b_2 = 0.0368$; $b_3 = 0.1434$. These two latter values are very close to the experimentally measured amplitude of C/C_0 between the depletion and concentration zones, and the relative

Table 1 Characteristics of five plinthite nuclei and the redoximorphic features surrounding them, sampled in sediments of lower Orinoco River at Mapire, Venezuela

Sample	Distance from nucleus surface (cm)	% Fe_2O_3	C/C_o^a	Fe_o/Fe_d^b	Munsell color
Sediment matrix	NA	0.59 ± 0.11	0.14	ND	10YR 7/1
Mean nucleus (C_o)	NA	5.51 ± 1.87	1.00		10YR 6/3
Structure A					
Nucleus	NA	2.99	1.00	0.36	10R 3/6
Ring 1 (C)[c]	4.7	1.05	0.21	0.23	10R 6/4
Ring 2 (D)[d]	7.9	0.60	0.12	0.16	10R 6/3
Ring 3 (C)	12.7	1.04	0.21	0.11	10R 5/6
Ring 4 (D)	17.4	0.77	0.15	0.24	10R 6/3
Structure B					
Nucleus	NA	8.23	1.0	ND	10R 3/4
Ring 1 (C)	1.1	2.26	0.45	ND	10R 4/6
Ring 2 (D)	4.8	0.92	0.18	ND	10R 4/4
Ring 3 (C)	6.4	1.11	0.22	ND	10R 5/6
Ring 4 (D)	8.7	0.49	0.10	ND	10YR7/1
Ring 5 (C)	14.0	0.42	0.08	ND	10R 5/3
Ring 6 (D)	19.4	0.42	0.08	ND	10YR5/3
Ring 7 (C)	22.6	0.65	0.13	ND	10R 5/6
Structure C					
Nucleus	NA	5.76	1.00	0.75	10R 3/6
Ring 1 (C)	3.9	1.24	0.25	0.20	10R 5/6
Ring 2 (D)	6.9	0.70	0.14	0.18	10R 6/4
Ring 3 (C)	9.4	1.10	0.20	0.26	10R 4/6
Ring 4 (D)	13.9	0.58	0.12	1.60	10YR7/1
Ring 5 (C)	16.4	0.80	0.16	0.36	10R 6/4
Structure D					
Nucleus	NA	5.48	1.00	1.02	10R 4/6
Ring 1 (C)	4.4	1.33	0.26	0.32	10R 3/6
Ring 2 (D)	8.7	0.73	0.14	0.30	10R 6/3
Ring 3 (C)	10.7	1.00	0.2	0.89	10R 4/6
Ring 4 (D)	12.4	0.81	0.16	0.41	10R 5/4
Ring 5 (C)	14.7	1.16	0.23	0.29	10R 4/6
Ring 6 (D)	18.2	0.57	0.11	0.44	5YR 6/2
Ring 7 (C)	19.9	0.97	0.19	0.52	10R 4/6
Structure E					
Nucleus	NA	5.08	1.00	0.34	10R 4/6
Ring 1 (C)	1.3	1.44	0.29	0.57	10R 4/8
Ring 2 (C)	2.2	1.29	0.26	0.26	10R 5/6
Ring 3 (C)	2.9	1.20	0.24	0.26	10R 5/6
Ring 4 (C)	3.2	1.07	0.21	0.26	10R 6/4
Ring 5 (C)	3.6	0.93	0.18	0.22	10R 5/4

Table 1 continued

Sample	Distance from nucleus surface (cm)	% Fe_2O_3	C/C_o[a]	Fe_o/Fe_d[b]	Munsell color
Ring 6 (D)	3.8	0.82	0.16	0.59	5YR 6/3

NA Not applicable, *ND* not determined

[a] Relative concentration of ferric oxide, calculated as the ratio of Fe_2O_3 concentration in each ring to the average Fe_2O_3 concentration of the nuclei (C_o)

[b] Fe_o/Fe_d refers to the ratio of oxalate- extracted Fe (amorphorous Fe) to the dithionite-extracted Fe (crystalline) forms of Fe

[c] (C), Concentration zone

[d] (D), Depletion zone

concentration of Fe_2O_3 in the sediment matrix away from the redoximorphic features, respectively. This empirical fit seems to conform both to the diffusive nature of the process as distance increases from the original source and to the forcing imposed by the flip-flop switch from reducing to oxic conditions regulated by river hydrology. In Fig. 4 the distance from the surface of the nucleus is shown along the x axis; this was calculated as the mean square displacement (random walk), $x = (2Dt)^{1/2}$, where x is the distance, D is the diffusion coefficient assumed for Fe^{2+} (1.03×10^{-6} cm^2 s^{-1}) and t is time. The mean distance between maxima, when $d(C/C_0)/x = 0$, is equivalent to 5.55 cm. This value is consistent with the mean square displacement of Fe^{2+} during 1.83×10^7 s, or 212 days.

Theoretically, a source of Fe, such as the nucleus, is subjected to reducing conditions when the river level is higher than the site of the nucleus and the oxygen concentration drops. At the location where these structures were found, the nuclei are submerged an average of 212 days every year. Here, we propose a three-component hypothetical mode of formation to explain the accretionary process over a distance as long as 30 cm from the nucleus. The mode of formation involves reduction to Fe^{2+}, diffusion and eventual oxidation to Fe^{3+}, and its partial crystallization, as modulated by the annual fluctuations in the river level. The oxidation potential of Fe^{2+} at pH 6 is 0.2 V. In previous studies carried out in the vicinity of the location in Orinoco, Vegas-Vilarrubia and Herrera (1993) reported a pH of 6.5 for Orinoco waters close to this study site; we also reported a stratification of the Orinoco water column starting in July, leading to a sharp decline in dissolved oxygen from over 6 mg L^{-1} near the surface to around 1 mg L^{-1} with depth, possibly reaching anoxia in the water–sediment interphase. Nitrite concentrations were also detectable in the deeper zones of the water column in August (NO_2^-–N ranged from 3.6 to 4.7 μg L^{-1}). Ferric iron is reduced under anaerobic conditions, probably mediated by microbial processes, and ferrous ions diffuse outward until the river level decreases again below the site; thus, oxidation ensues, followed by partial precipitation as ferric oxide. Ahmad and Nye (1990) suggested that this latter process is fast and independent of pH when it occurs on newly formed adsorption surfaces of ferric oxides. This process is usually considered to be mediated by microorganisms through microbial dissimilatory Fe reduction (Munch and Otto 1980; Beard et al. 1999, 2003; Cornell and Schwertmann 2003; Chan et al. 2006; Crosby et al. 2005, 2007). Under atmospheric conditions, Fe(III) is the thermodynamically stable oxidation state. However, when exposed to air, the released Fe(II) is rapidly oxidized, followed by the precipitation of poorly

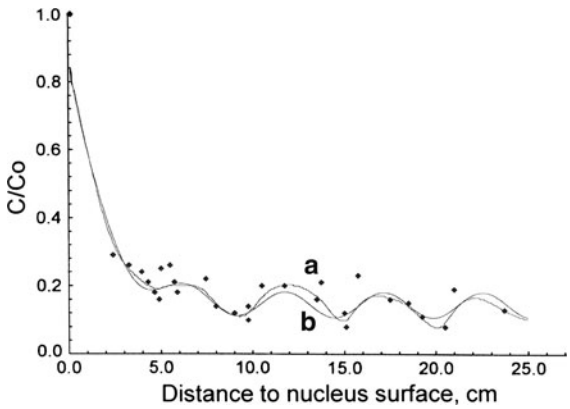

Fig. 4 Normalized total Fe concentrations as a function of distance from the nucleus surface in the five redoximorphic structures analyzed. A smoothing quadratic spline was calculated; this is shown as curve *a*. Curve *b* was calculated as the best fit (Eq. 1). *Dots* represent experimental data (see text)

crystalline Fe oxyhydroxide minerals, such as ferrihydrite. Reduction is thought to proceed faster from amorphous Fe oxides (Wiederhold et al. 2007). The transformation to crystalline Fe oxide minerals, such as goethite and hematite, takes place during further wet and dry cycles. These diffusion/precipitation processes seem to occur annually following the river-level fluctuation pattern. Newly formed ferric oxide accumulations away from the nucleus would then act as secondary sources from where further reduction to Fe^{2+} and diffusion occurs. Wu et al. (2010) recently successfully demonstrated how stable Fe-isotope fractionations can be used to investigate changes in surface Fe phases during the exposure of Fe(III) oxides to aqueous Fe(II) under different environmental conditions. Their results confirm the coupled electron and atom exchange mechanism proposed to explain Fe isotope fractionation during dissimilatory iron reduction (DIR). They also compared this biologically mediated mechanism to the non-biological processes which they deem to be less efficient in many natural systems.

Effects of ENSO

In April 1996, after a strong El Niño event (ENSO) immediately followed by a strong La Niña year, the river dropped to about 11 m a.s.l., allowing us to observe two additional fields of redoximorphic structures in the sediment that is usually exposed to air for much shorter periods. In field b (Fig. 2) at 12.5 m a.s.l. we found narrower but more widely spaced ferric rings, with each ring having a distinct banded structure. Average spacing between rings at this field was 7.3 ± 1.2 cm ($n = 14$). A few larger concentric rings of a purple color were also observed at distances between 22 and 96 cm from the nucleus. The purplish color and the longer distance from the nuclei suggest that they might be due to manganese (Mn) precipitation in a similar process as the one described for Fe. Annual exposure to the air is very brief (a few days each year). The presence of RFs at the site (field b) where there are annual but short intervals of oxidizing conditions fits well with the expected value calculated for $t = 2.6 \times 10^7$ s or 299 days. This figure is consistent with the average annual floods that can be observed in Fig. 2.

In field c (Fig. 2) which is further below, at approximately 11.5 m a.s.l., fewer nuclei were found surrounded by single, very fine reddish rings. The sediment surface at this height (Fig. 2, field c) is only exposed to the air when a strong river-level anomaly occurs associated to ENSO effects. The average radial distance between the nuclei and concentric rings measured was 11 ± 3 cm ($n = 8$). The larger spacing in the lowest site (field c) corresponds to average flood times of around 9.4×10^7 s or nearly 3 years under flood conditions. Although strong ENSO events do not occur at fixed intervals, data from National Oceanic and Atmospheric Administration (NOAA) show that between 1950 and 2010 the mean observed return period was 2.41 ± 0.86 year ($n = 19$) for El Niño and 2.61 ± 1.5 year ($n = 17$) for La Niña (http://www.esrl.noaa.gov/psd/people/klaus.wolter/MEI/). García and Mechoso (2005) found that time-series of streamflows for the Orinoco River show an ENSO-like periodicity of about 4.5 years as well as a quasi-biennial oscillation with a period of about 2.5 years.

Long-term ENSO effects and forecasts of river hydrology have also been analyzed using tree rings as proxy (Schöngart et al. 2004; Schöngart and Junk 2007) elsewhere in South America. A relatively shorter term correlation between flood duration and annual tree-ring formation was found in a seasonally flooded forest at the same location in the Orinoco floodplains (Dezzeo et al. 2003). Inasmuch as tree rings represent a purely biological growth process while redoximorphic features in river sediments are dominated by physicochemical processes, possibly mediated by biological ones, a more detailed study of how both processes respond to wetter or drier than average years may improve our understanding of the coupling between climate, river fluctuation, and their effects on the surrounding terrain and vegetation, possibly at complementary time-scales.

Conclusions

The characteristics of the structures discovered in the sediments of Orinoco River, their composition and mineralogy, and their spatial organization can be interpreted to be the result of repeated cycles of alternating redox conditions imposed by river hydrology. Here we suggest a possible mode of their formation using the switch to reducing conditions and diffusion of soluble Fe during periods of flood, its subsequent oxidation and hence immobilization, and its partial crystallization once exposed to the air.

As a first approximation in the understanding of the nodules and redoximorphic features discovered in Orinoco, we propose a simple hypothetical mode of accretion that could explain the formation of these concentric ring structures as follows:

- Starting with a discrete iron-rich plintite nucleus embedded in a porous matrix of low Fe content
- Iron in the nucleus surface is reduced through a microbial-mediated process when the nucleus is flooded: $Fe^{3+} \rightarrow Fe^{2+}$
- During the flood period Fe^{2+} moves away from the source following diffusion according to Fick's Laws and thus producing depletion zones.
- When the flood recedes, oxidation proceeds, fixing some of the mobilized Fe^{3+} into a ring at a distance dictated by diffusion.
- Partial crystallization of Fe_2O_3 occurs during the ensuing dry period
- When the water level once again covers the nucleus and the surrounding structure, a fraction of Fe^{3+} is again reduced to Fe^{2+} which is diffused away giving rise to depletion zones.
- The repetition of this process through the seasonal river cycle would give rise to the concentric ring structure of the observed redoximorphic features.
- These structures should then respond to both seasonal mean river fluctuations and to ENSO- or NAO-induced anomalies which maintain the site under flood for varying periods.

This proposed mode of formation presents some similarities to periodically distributed nucleation and Liesegang banding formed by the interdiffusion of Fe^{2+} and O_2 in porous media (Chan et al. 2000). The role of microorganisms in these processes and the interactions between the biogeochemical cycle of Fe and phosphorus (P), organic C, and aluminum (Al) needs further clarification. Chacón et al. (2005, 2006, 2008) report significant interactions in the cycles of those elements in soils of the Orinoco River floodplain in the Mapire floodplain in the vicinity of our site (Fig. 1).

The rate of formation of these RFs is not known. They may represent a long series of repeated cycles following the river-level seasonality, with each cycle leaving an additional front producing in time a coalescence that appears as thicker Fe-concentration zones. Two approaches can be taken to study accretion rates: reproducing a similar process under controlled laboratory conditions or modeling, as has been done for self-organized precipitates in concretions in the Navajo Sandstones (Chan et al. 2007; Barge et al. 2011). Chan et al. (2004) in a comparative study of spherical hematite concretions on Mars and similar structures in Navajo Sandstone conclude that the formation of such RFs requires the presence of a permeable matrix, groundwater flow, and a chemical reaction front. In the case of our study of RFs in the Orinoco sediments, the first two requirements are clearly met and the latter could be inferred due to the quasi-regularity of the river dynamics.

Acknowledgments This work was financed entirely by the Venezuelan Institute of Scientific Research, IVIC. The authors dedicate this paper to the memory of Professor Dr. Richard Schargel (1938–2011). The contribution of two anonymous reviewers is gratefully acknowledged. We wish to express our gratitude to Mr. J. L. Vallés, Drs. M. Bezada, and L. D. Llambí for their assistance during the fieldwork, to Ms. G. Escalante, Mr. L. Lado, and D. Benzo for help with some of the analyses, and to Professor M. Puma and Dr. M. Lampo for their help with data processing and graphics. We also wish to thank Professors F. García-Golding, S. Glatzel, and A. Lidón for critical discussions of earlier versions of this manuscript and to Ms. A. Angulo for proof-reading the final version.

References

Ahmad AR, Nye PH (1990) Coupled diffusion and oxidation of ferrous iron in soils. I. Kinetics of oxygenation of ferrous iron in soil suspension. J Soil Sci 41:395–409

Asikainen CA, Werle SF (2007) Accretion of ferromanganese nodules that form pavement in Second Connecticut Lake New Hampshire. Proc Natl Acad Sci USA 104(45):17579–17581

Atkins JE, McBride EF (1992) Porosity and packing of Holocene river, dune and beach sands. Am Assoc Pet Geol Bull 76:339–355

Barge LM, Hammond DE, Chan MA, Potter S, Petruska J, Nealson KH (2011) Precipitation patterns formed by self-organizing processes in porous media. Geofluids 11(2): 124–133

Beard BL, Johnson CM, Cox L, Sun H, Nealson KH, Aguilar C (1999) Iron Isotope biosignatures. Science 285:1889–1892

Beard BL, Johnson CM, Skulan JL, Nealson H, Cox L, Sun H (2003) Application of Fe isotopes to tracing the geochemical and biological cycling of Fe. Chem Geol 195: 87–117

Borgaard O (1979) Selective extraction of amorphous iron oxides by EDTA from a Danish sandy loam. J Soil Sci 30:727–734

Carbón J, Schubert C (1994) Late Cenozoic history of the eastern llanos of Venezuela: geomorphology and stratigraphy of the Mesa Formation. Quatern Int 21:91–100

Chacón N, Dezzeo N, Muñoz B, Rodríguez JM (2005) Implications of soil organic carbon and the biogeochemistry of

iron and aluminum on soil phosphorus distribution in flooded forests of the lower Orinoco River, Venezuela. Biogeochemistry 73:555–566
Chacón N, Flores S, González A (2006) Implications of iron solubilization on soil phosphorus release in seasonally flooded forests of the lower Orinoco river, Venezuela. Soil Biol Biochem 38:1494–1499
Chacón N, Dezzeo N, Rangel M, Flores S (2008) Seasonal changes in soil phosphorus dynamics and root mass along a flooded tropical forest gradient in the lower Orinoco river, Venezuela. Biogeochemistry 87:157–168
Chan MA, Parry WT, Bowman JR (2000) Diagenetic hematite and manganese oxides and fault-related fluid flow in Jurassic sandstones, southeastern Utah. AAPG Bull 84:1281–1310
Chan MA, Beitler B, Parry WT, Ormö J, Komatsu G (2004) A possible terrestrial analogue for hematite concretions on Mars. Nature 429:731–734
Chan MA, Johnson CM, Beard BL, Bowman JR, Parry WT (2006) Iron isotopes constrain the pathways and formation mechanisms of terrestrial oxide concretions: a tool for tracing iron cycling on mars? Geosphere 2(7):324–332. doi:10.1130/GES00051.1
Chan MA, Ormo J, Park AJ, Stich M, Souza-Egipsy V, Komatsu G (2007) Models of iron oxide concretion formation: field, numerical and laboratory comparisons. Geofluids 7: 356–368
Cornell RM, Schwertmann U (2003) The iron oxides: structure, properties, reactions, occurrence and uses, 2nd edn. VCH, Weinheim
Crosby HA, Johnson CM, Roden EE, Beard BL (2005) Coupled Fe(II)–Fe(III) electron and atom exchange as a mechanism for Fe isotope fractionation during dissimilatory iron oxide reduction. Environ Sci Technol 39:6698–6704
Crosby HA, Roden EE, Johnson CM, Beard BL (2007) The mechanisms of iron isotope fractionation produced during dissimilatory Fe(III) reduction by *Shewanella putrefaciens* and *Geobacter sulfurreducens*. Geobiology 5:169–189
Dezzeo N, Worbes M, Ishii I, Herrera R (2003) Annual tree rings revealed by radiocarbon dating in seasonally flooded forest of the Mapire River, a tributary of lower Orinoco, Venezuela. Plant Ecol 168:165–175
Fimmen RL, de Richter DB, Vasudevan D, Williams MA, West LT (2008) Rhizogenic Fe–C redox cycling: a hypothetical biogeochemical mechanism that drives crustal weathering in upland soils. Biogeochemistry 87:127–141
García NO, Mechoso CR (2005) Variability in the discharge of South American rivers and in climate. Hydrol Sci J 50: 459–478
Gasparatos D, Tarenidis D, Haidouti C, Oikonomou G (2005) Microscopic structure of soil Fe-Mn nodules: environmental implication. Environ Chem Lett 2:175–178
Gee GW, Bauder JW (1986) Particle-size analysis. In: Knute A (ed) Methods of analysis, part 1. Physical and mineralogical methods. Agronomy monograph no. 9. Soil Science Society of America, Madison, pp 383–411
Jackson ML (1958) Soil chemical analysis. Prentice-Hall, Englewood Cliffs
Kirk GJD, Ahmad AR, Nye PH (1990) Coupled diffusion and oxidation of ferrous iron in soils. II. A model of diffusion and reaction of O_2, Fe^{2+}, H^+ and HCO_3^- in soils and sensitivity analysis of the model. J Soil Sci 41:411–431
Labat D, Ronchail J, Guyot JL (2005) Recent advances in wavelet analyses: part 2-Amazon, Parana, Orinoco and Congo discharges time scale variability. J Hydrol 314: 289–311
Lelong F (1966) Régime des nappes phréatiques continues dans la formations d'alteration tropicale. Consequences pour la pédogénese. (Water-table continuous regimes and the formation of alterites in tropical soils. Its consequences on pedogenesis (in French). Sci Terre 11:203–244
Lewis WM, Saunders JF (1989) Concentration and transport of dissolved and suspended substances in the Orinoco River. Biogeochemistry 7:203–240
Mehra O, Jackson M (1960) Iron oxide removal from soils and clays by dithionite-citrate system buffered with sodium carbonate. Clays Clay Miner 7:317–327
Munch J, Otto J (1980) Preferential reduction of amorphous to crystalline iron oxides by bacterial activity. Soil Sci 129: 15–21
Nieto R, Gallego D, Trigo R, Ribera P, Gimeno L (2008) Dynamic identification of moisture sources in the Orinoco basin in equatorial South America. Hydrol Sci J 53(3): 602–617
Paolini J (1995) Particulate and organic carbon and nitrogen in the Orinoco River (Venezuela). Biogeochemistry 29:59–70
Parry WT (2011) Composition, nucleation, and growth of iron oxide concretions. Sed Geol 233(1–4):53–68
Poveda G, Mesa OJ (1997) Feedbacks between hydrological processes in Tropical South America and large-scale ocean—atmospheric phenomena. J Clim 10:2690–2702
Poveda G, Waylen PR, Pulwarty RS (2006) Annual and inter-annual variability of the present climate in northern South America and southern Mesoamerica. Palaeogeogr Palaeoclimatol Palaeoecol 234:3–27
Rodríguez-Altamiranda R, Flores S, Herrera R (2011) Gestión sostenible del bosque inundable mediante la participación comunitaria en Mapire. Anzoátegui, Venezuela. In: Herrera FF, Herrera I (eds) Regeneración de Ecosistemas en Venezuela. Ediciones IVIC, Caracas, pp 149–165
Schöngart J, Junk WJ (2007) Forecasting the flood-pulse in Central Amazonia by ENSO-indices. J Hydrol 335:124–132
Schöngart J, Junk WJ, Piedade MTF, Ayres JM, Hüttermann A, Worbes M (2004) Teleconnection between tree growth in the Amazonian floodplains and the El Niño-Southern Oscillation effect. Glob Change Biol 10:683–692
Sivarajasingham S, Alexander L, Cady J, Cline M (1962) Laterite. Adv Agron 14:1–60
Sommers MG, Dollhopf ME, Douglas S (2002) Freshwater ferromanganese stromatolites from Lake Vermilion, Minnesota: microbial culturing and environmental scanning electron microscopy investigations. Geomicrobiol J 19: 407–427
Spicar E (2004) Egendomliga bildningar I Dalasandstenen (Peculiar structures in sandstones of Dalarna (in Swedish). Geologiskt For 44:18–25
Stolt M, Ogg C, Baker C (1994) Strongly contrasting redoximorphic patterns in Virginia valley and ridge paleosols. Soil Sci Am Soc J 58:477–484
Thomaz SM, Bini LM, Bozelli RL (2007) Floods increase similarity among aquatic habitats in river-floodplain systems. Hydrobiologia 579:1–13. doi:10.1007/s10750-006-0285-y

Thompson A, Chadwick OA, Boman S, Chorover JO (2006a) Colloid mobilization during soil iron redox oscillations. Environ Sci Technol 40:5743–5749

Thompson A, Chadwick OA, Rancourt DG, Chorove J (2006b) Iron-oxide crystallinity increases during soil redox oscillations. Geochim Cosmochim Acta 70:1710–1727

van Wambeke A, Eswaren H, Herbillon AJ, Comerma J (1983) Oxisols. In: Wilding LP et al. (eds) Pedogenesis and soil taxonomy: II. the soil orders. Elsevier, New York, pp 325–354

Vegas-Vilarrubia T, Herrera R (1993) Effects of periodic flooding on the water chemistry and primary production of the Mapire river system (Venezuela). Hydrobiologia 262: 31–43

Vepraskas M (1992) Redoximorphic features for identifying aquic conditions. NC Agric Res Serv Tech Bull 301. NC Agricultural Research Service, Raleigh

Vepraskas MJ, Faulkner SP (2000) Redox chemistry of hydric soils. In: Richardson JL, Vepraskas MJ (eds) Wetland soils: genesis hydrology landscapes and classification. Lewis, Boca Raton, pp 85–107

Wiederhold JG, Teutsch N, Kraemer SM, Halliday AN, Kretzschmar R (2007) Iron isotope fractionation during pedogenesis in redoximorphic soils. Soil Sci Soc Am J 71(6):1840–1850

Wu L, Beard BL, Roden EE, Kennedy CB, Johnson CM (2010) Stable Fe isotope fractionations produced by aqueous Fe(II)-hematite surface interactions. Geochim Cosmochim Acta 74(15):4249–4265